Journal of Applied Polymer Science

ForceSpinning of polyacrylonitrile for mass production of lithium-ion battery separators

Victor A. Agubra, David De la Garza, Luis Gallegos, Mataz Alcoutlabi
Department of Mechanical Engineering, University of Texas-Pan American, Edinburg, Texas
Correspondence to: M. Alcoutlabi (E-mail: alcoutlabimy@utpa.edu or mataz.alcoutlabi@utrgv.edu)

ABSTRACT: We present results on the Forcespinning® (FS) of Polyacrylonitrile (PAN) for mass production of polymer nanofiber membranes as separators for Lithium-ion batteries (LIBs). Our results presented here show that uniform, highly fibrous mats from PAN produced using Forcespinning®, exhibit improved electrochemical properties such as electrolyte uptake, low interfacial resistance, high oxidation limit, high ionic conductivity, and good cycling performance when used in lithium ion batteries compared to commercial PP separator materials. This article introduces ForceSpinning®, a cost effective technique capable of mass producing high quality fibrous mats, which is completely different technology than the commonly used in-house centrifugal method. This Forcespinning® technology is thus the beginning of the nano/micro fiber revolution in large scale production for battery separator application. This is the first time to report results on the cycle performance of LIB-based polymer nanofiber separators made by Forcespinning® technology. © 2015 Wiley Periodicals, Inc. J. Appl. Polym. Sci. **2016**, *133*, 42847.

KEYWORDS: batteries and fuel cells; electrochemistry; membranes; nanostructured polymers

Received 17 June 2015; accepted 17 August 2015
DOI: 10.1002/app.42847

INTRODUCTION

As the lithium-ion battery becomes the preferred battery chemistry for most portable energy applications, so has the demand for continuous improvement in its components to meet the optimum battery performance at various operating conditions. The separator, whose main function is to keep the positive and negative electrodes apart in order to prevent electrical short circuits while allowing rapid transport of ionic charge carriers across the interface, has received considerable research attention recently. Most of the research reported on LIB separators is geared towards their design and development with the aim to improve the overall electrochemical performance of LIBs.[1–5] A majority of the separators currently used in LIBs are those typically developed as spin-offs of existing technologies and not designed specifically for a particular battery chemistry.[6] Therefore most often than not, these separators are not completely optimized for use as separators for LIBs. This approach however, drives down the cost component of producing the separator. Polymeric nanofiber membranes in recent times have seen extensive research activities for their use as alternate separators in Li-ion batteries due to their large porosity, unique pore structure, and high electrolyte uptake.[7–11] These nanofibers can be produced by several methods such as electrospinning,[12,13] electrospray, wet laid, melt blowing, and microwave-assisted processes. However, these methods have some drawbacks, such as low spinning rate and high production cost.[14–16] These drawbacks make these separator materials rather unattractive for lithium ion battery applications.

Polyolefin microporous membranes such as polyethylene (PE) and polypropylene (PP) are commercially available and have been widely used as separators for LIBs because of their good thermal shutdown ability, electrochemical stability and high mechanical strength.[17,18] However, these polyolefin-based separators show low porosity, poor electrolyte wettability and high thermal shrinkage at relatively elevated temperatures above 90°C. Several approaches have been used to overcome these drawbacks including the use of nanoparticle composite additives, coating the membrane separator with a polymer NFs (e.g. PVDF) and/or the use of nonwoven and nanofiber-based separators.[19–22] The latter approach is very promising and has been widely used due to the fact that NF-based separators exhibit good electrolyte uptake, low interfacial resistance but they show poor mechanical strength which render them difficult to handle during battery-assembly operation.[23,24]

The commonly used separators in lithium-ion batteries are the microporous polyolefin, polypropylene, polyethylene, polyvinylidene difluoride (PVdF) separator or PVdF-coated microporous polyolefin separators.[25–27] Several companies such as Celgard, Asahi, Toray, Entek Membrane, Ube industries, DSM, etc. have designed and developed commercial separators for the over $4billion lithium ion batteries market,[5] these mostly consist of polymer materials such as polyolefin microporous membranes developed

by Celgard, DSM, and Asahi and a tri-layer of polypropylene/polyethylene/polypropylene from Celgard and Ube industries. Most of these companies are looking to design separators with (1) more porosity, (2) safer to puncture and shorts, (3) higher melt stability, (4) thinner structure to allow for more active material, (5) very thin layer to allow for composite structures of ceramic coatings, (6) very thin and porous nonwoven to be filled with polymer electrolyte, (7) High thermal stability, and (8) lower cost for used in hybrid vehicles automobile.[5,25,27] However, several studies[27–33] have pointed to these polymer-based battery separators to having less impressive key performance indices such as: high interface resistance, low thermal stability, and low electrolyte uptake. Polymers in general are known for their high thermal expansion coefficient[34] leading to high residual stresses after a change in operating temperature.[35] Hence the severe thermal shrinkage of polyolefin separators after a change in temperature can cause serious internal electrical short circuit leading to a fire disaster or battery explosion when the cells are exposed to abnormal operating conditions. Celgard have made several improvement to its PP mono layer polymer separator by designing a three layer separator comprising of the polypropylene/polyethylene/polypropylene thereby improving the deficiency of its mono layer separators Celgard.[36–42] As many researchers identify the short comings of these microporous polymer separators, have paved the way for many research efforts aimed at improving their electrochemical performance. Some of these research efforts include; coating the microporous polymer separators with ceramics like TiO_2 on the Tri-layer polymeric separator,[27] Al_2O_3 and hydrophilic poly(lithium-4-styrenesulfonate) onto the porous polyethylene membrane,[33] and SiO_2 coating on polyethylene.[43,44] These ceramic coating on the polymeric separator not only afford the separator its dimensional stability, but they also improve the porous structure of the separator that allow higher ion transport to improve ionic conductivity and low internal resistance.[11,45] The nonwoven nanofibers have also seen a share of research activities as an alternate separator materials for lithium ion batteries applications.

The nonwoven fiber mat separators are typically thick (i.e., 100–200 μm); however, in effort to reduce this thickness, recent fiber manufacturing technology such electrospinning, centrifugal spinning, and ForceSpinning® have emerged that can produce fiber of thickness of 10−20 μm with diameters that are typically less than 5 μm.[11,46–50] These fiber processing methods have been successful in giving the nonwoven separators its high labyrinth-like pores structure.[48] Presently the most commonly used methods for making these nanofibers employ either an electrostatic charge (electrospinning)[51] or external heated air jets (melt-blowing),[40,52–56] bicomponent fiber spinning, phase separation, template synthesis, and self-assembly. These methods are often complex and can only be used to make nanofibers from limited types of polymers, often lab-scale in nature and cannot be used for large scale manufacturing due to the associated cost.

Centrifugal spinning, that basically mimics the ForceSpinning principle, has been used to make nanofibers for both battery and other applications and many articles are now being published after Lozano *et al.* at UTPA long obtained a patent and a spun-off company was established.[15] However, the centrifugal spinning method, has several drawbacks such as; it cannot be used to produce fibers of uniform cross-section, it has no capacity of melt spinning, thus it incapable of producing fibers from very viscous solutions and a very low fiber yield.[50,57–59] The ForceSpinning Technique, on the other hand, has several features such as a fiber management system that allow tunable fiber deposition to ensure accurate cross directional coating uniformity, and also adaptable to substrate web widths. The FiberLab L1000 system in particular, has the capability for dual materials feed thus allowing the continuous materials feed system especially for melt and solution processing with no material dielectric properties requirements.[60] Additionally, the FiberLab L 1000 has an almost 100% yield and solvent-free processing for melt spinning with melt temperatures up to 350°C. This eliminates the direct operating expense and environmental burdens and thus allowing a fiber yield greater than 60 g/h much higher than the in-house built centrifugal method.

In this article, we focus on the use of Forcespinning method for the mass production of nonwoven PAN nanofiberous mats as separators for LIBs. The nanofibers produced by this method are uniform, porous, and exhibit good electrochemical properties thus making them better candidates for commercial lithium-ion battery separators. The ForceSpinning method will thus revolutionize the production of nonwoven nanofibers as alternate battery separators for commercial lithium ion batteries.

EXPERIMENT

Materials

Poly(acrylonitrile) with average M_w 150,000 was purchased from Sigma Aldrich USA, while solvent *N,N*-dimethyl Formamide (DMF) was obtained from Fisher Scientific USA. The commercial LiFePo4, the lithium foil, and the lithium hexafluorophosphate (LiPF6), ethylene carbonate (EC), dimethyl carbonate (DMC), were purchased from MTI corp. USA, while the PP mono layer separator was used as received from Celgard, USA.

Methods

The production of the PAN nanofiber was performed using the Forcespinning® FiberLab L1000 (FibeRio). The characterization of the force spun membranes was done using the Scanning Electron Microscope and transmission scanning electron microscopy (STEM) with a Sigma VP Carl Zeiss, Germany. The preparation $LiFePO_4$/Li cells with PAN nanofibers were performed in a glove box (Mbraun, USA) filled with high purity Argon. The ionic conductivity as well as the oxidation limits of the PAN and PP were evaluated using electrochemical impedance spectroscope (Autolab 128N), while the electrochemical cycling performance of the cells was performed in a battery test station from Arbin Instruments, USA. Differential scanning calorimetry (DSC) was performed using DSCQ100 and sample average weight of about 10 mg were used in the DSC experiments which were performed at a heating rate of 5°C/min heating up to 300°C.

Forcespinning of PAN Fibrous Membranes

The poly(acrylonitrile) was dissolved in DMF by magnetic stirring at 60°C in a silicon oil bath to obtain a homogenous solution of concentration of 12 wt %. The Fibrous membranes of PAN were prepared by forcespinning method when the solution was cooled to room temperature. A thin fiber cloth was used on a fan box as the substrate for deposition of fibers. In the FS technique,

centrifugal force is used to extrude polymer solutions or melts. Fiber jets are formed by high rotational speeds of a spinneret. The rotation of the spinneret has speeds up to 20, 000 rpm which drives the fluid through the needle orifices. For the PAN solution, an amount 2 mL of the solution were injected into the needle-based spinneret equipped with 30 gauge half-inch regular bevel needles. The rotational speed of the spinneret was kept at 8,000 rpm. The substrate was rotated 90° after each run and the needles either cleaned or change entirely. In each experiment, 12 runs were performed to obtain a mat thickness of about 26 μm thickness. The forcespun PAN membrane mat was removed from the substrate drum and dried at 100°C under vacuum for 24 h prior to being used. The mat thickness was measured by taking a cross section view using the STEM. Surface morphology, thermal stability, and electrolyte uptake capacity experiments were performed to characterize the PAN membrane separators. The fiber production procedure is illustrated in the Figure 1.

Physical and Electrochemical Characterization

The electrolyte uptake performance of the dry PAN membrane and the PP mircroporous membrane separators were evaluated by performing the liquid electrode uptake (EU) measurements. This was conducted according to ASTM D570, the dry membranes were weighed and subsequently immersed in the liquid electrolyte of 1*M* LiPF6 in EC:DMC (1:1 by volume) for 10 min at room temperature, followed by being weighing after removing the surface liquid with filter paper. The EU was then computed using the following equation:

$$EU(\%) = \frac{W - W_0}{W_0} \times 100$$

Where W_0 and W are the weights of the membranes before and after soaking in the electrolyte, respectively.

The electrolyte uptake capacities on the other hand were evaluated by first soaking the dry weighted PAN membrane and PP Celgard separator into the 1*M* LiPF6 in EC:DMC (1:1 by volume) at room temperature for a specific time interval. Any excess electrolyte solution on the separator was gently wiped off with a filter paper. The electrolyte uptake capacities were then computed using the following equation:

$$\text{Uptake capacity } \left(\frac{\text{mg}}{\text{cm}^2}\right) = \frac{W - W_0}{A}$$

where W and W_o are as defined in eq. (1) while A is the surface areas of the separator. The ionic conductivity of the PAN nanofiber membrane was evaluated at room temperature using the Autolab electrochemical analyzer. The PAN nanofiber membrane was placed in between the Lithium metal electrode and $LiFePO_4$ electrode (half-cell configuration) and the resistance (R, ohm) measurements were performed over the frequency range of 1 MHz to 1 kHz at amplitude of 10 mV. Ionic conductivity (σ) of the sample was calculated using the relationship:

$$\sigma = \frac{L}{RA} \quad (3)$$

where "L" is the thickness of the PAN membrane "A" is the cross sectional area, and R the ohmic resistance value taken from the Nyquist plots at the Z' axis intercept. The linear sweep voltammetry (LSV) test was also carried out to evaluate the oxidation limit of both the PAN and PE separators in the redox environment of the lithium ion battery. The parameters used for the LSV were: voltage range 2.5 V to 6.0 V, and a scan rate 1 mV/s.

The suitability of the forcespun PAN membrane as a separator for lithium-ion cell was tested by assembling and evaluating coin cell CR2032 cell, with commercially obtained $LiFePO_4$ (from MTI) as the working electrode and Lithium metal foil the counter electrode, with electrolyte made of 1 M $LiPF_6$ in EC:DMC (1:1). The assembled cells were evaluated for electrochemical performance with charge–discharge cycling between 2.0 Vand 4.0 V at current density of 50 m Ag^{-1} at room temperature.

RESULTS AND DISCUSSION

Separator Morphology

The morphology and structure of PAN membrane separator has a direct effect on its electrochemical properties and performance in the lithium ion battery. The fibrous structure of the PAN membrane plays a key role in its ion transport and conductivity behavior. Figure 2 shows SEM micrographs of the PAN membrane that are bead-free and fibrous in structure with large amount of mirco-pores [Figure 2(c)] and average fiber diameters are of <4 μm. Factors such as viscosity, surface tension, solution concentration had a direct influence on the fiber diameters of the Forcespun® fibers; however, the effect of these factors were minimized through heating of the solution in the silicon oil bath, choosing the appropriate needle gauge (i.e., 30Gx $\frac{1}{2}''$), and the spinneret speed. The observed results are in line with many other findings reported in literature for PAN and other polymeric fiber membranes.[61,62]

It has been well established that high porosity is beneficial for membrane separators because it helps absorb large amount of liquid electrolyte and by extension allows fast ion transportation between two electrodes.[39] The electrolyte uptake results shown in Figure 3(a), showed that the PAN membrane has a large mass electrolyte uptake of about 328% compared to the PP Celgard separator value of 82%. This difference in the two separators electrolyte uptake results stem from the porous and fibrous structure of the PAN membrane. The pores in the PAN membrane lock up the electrolyte and help in the electrolyte retention capacity of the membrane. A suitable separator for lithium ion batteries is required to rapidly absorb electrolyte in less than 60 s in order to be saturated,[63] the electrolyte uptake thus is a measure of how quickly a separator absorbs and reaches saturation point. The Electrolyte uptake capacity results [Figure 3(b)] shows that both the PP monolayer separator and the PAN membrane electrolyte capacities increase quickly for the first 20 s. However, that for the PAN membrane was higher than the PP Celgard separator, reaching a capacity of about 4.8 g cm^{-2} compared with 1.2 g cm^{-2} for the PP monolayer. This remarkable electrolyte capacity of the PAN membrane is often attributed to the presence of the polar groups on the backbone of the PAN molecule, thus making the PAN membrane a better electrolyte retention performer. The results on the electrolyte uptake of PAN NF mats [Figure 3(a,b)] are presented in two different fashions. Figure 3(a) is the electrolyte mass uptake, which is a measure of how quickly a separator

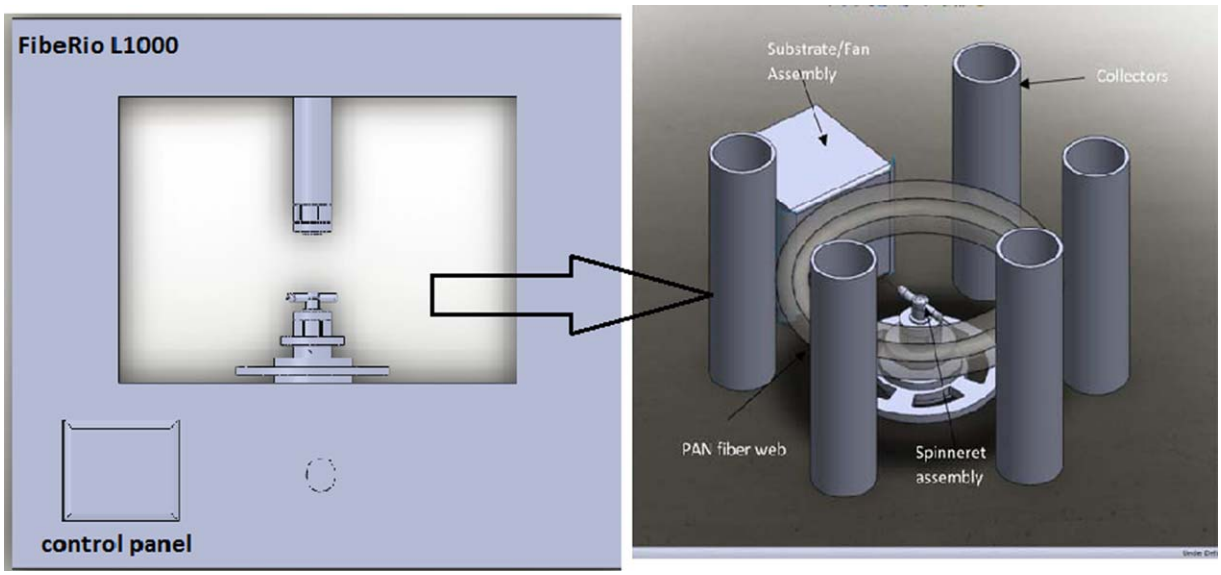

Figure 1. A pictorial view of the Forcespinning® machine and a schematic drawing of a typical setup inside the machine showing the collectors, the spinneret and the substrate/fan assembly for fiber production. [Color figure can be viewed in the online issue, which is available at wileyonlinelibrary.com.]

absorbs and reaches saturation point, a key performance index that indicate the wettability of the separator. The electrolyte capacity [Figure 3(b)] on the other hand, is an indication on how much electrolyte can be absorbed by the unit area of a separator membrane.

The comparative results of the electrolyte uptake and the electrolyte capacity indicated that the PAN membrane exhibited a higher electrolyte capacity than PP monolayer membrane. The electrolyte uptake, which is a measure of the amount of liquid electrolyte absorbed per unit area of the membrane, is one key performance index of a good lithium ion battery separator. It is worthwhile to mention that, the electrolyte uptake capacity of any separator membrane depends on the membrane microstructure properties such as thickness, porosity, and pore size. In this regard, a thin membrane with high porosity and pore size will have a higher

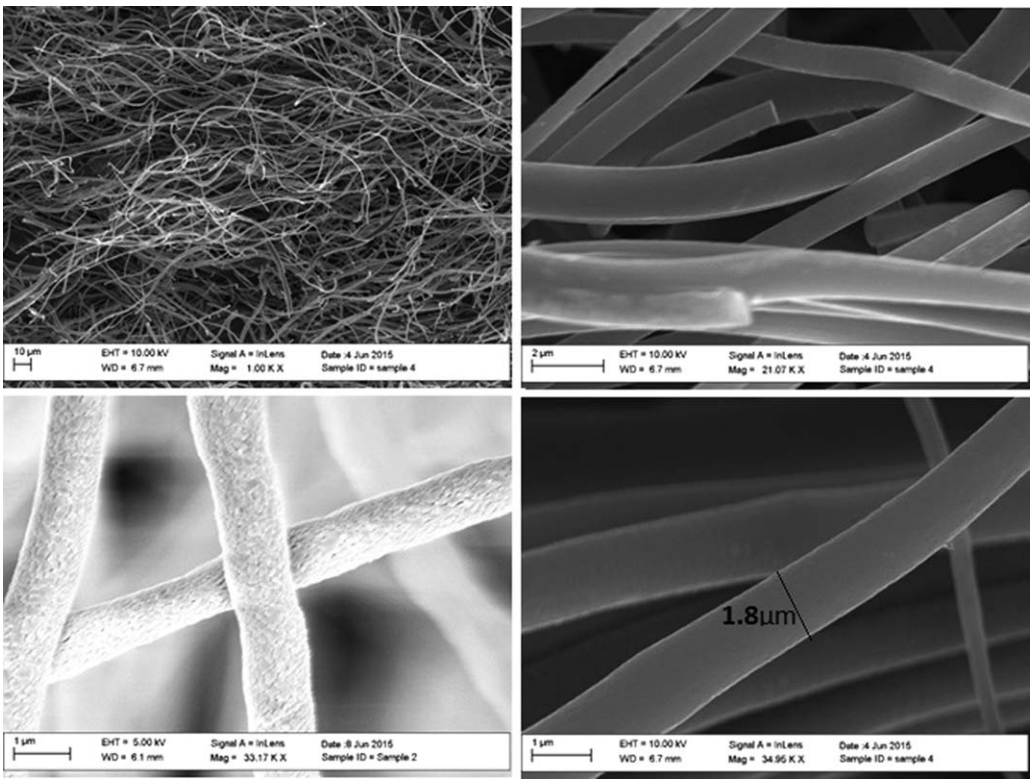

Figure 2. SEM micrographs showing the fibrous PAN membrane mat (a) with fiber average diameter of <2µm (d) and fiber with a lot of pores in them (c).

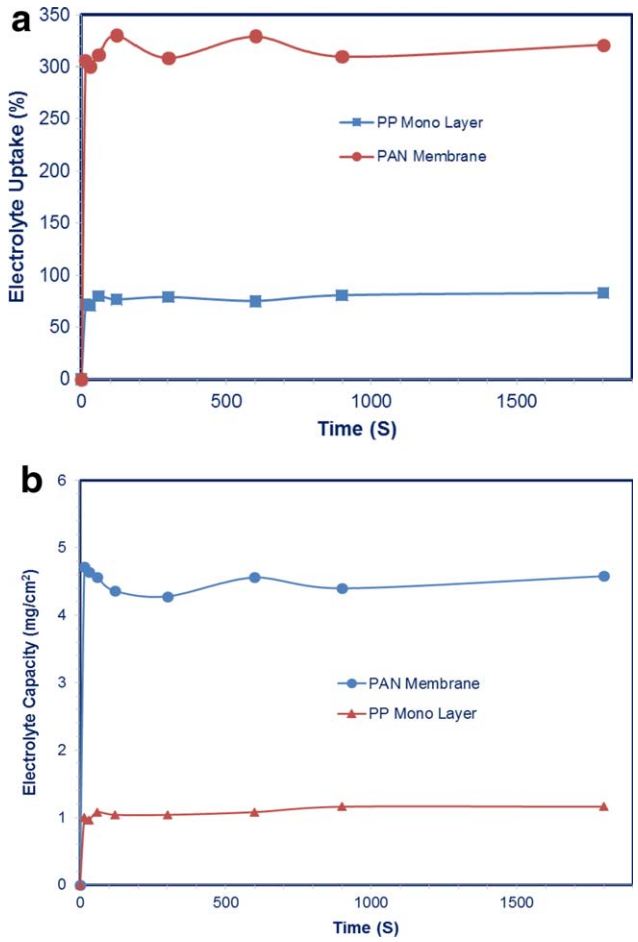

Figure 3. (a) Electrolyte mass uptake as a function of time for the PP mono layer separator and the PAN membrane. (b) Electrolyte uptake capacity as a function of time for the PP Celgard separator and the PAN membrane. [Color figure can be viewed in the online issue, which is available at wileyonlinelibrary.com.]

electrolyte capacity than thicker membrane with low porosity and pore size (higher weight).[36–39] To further elucidate, the effects of membrane microstructural properties like; porosity, pore size and

Table I. Physical Properties of PAN and PP Monolayer Separator

Separator	Electrolyte uptake (%)	Ionic conductivity (mS/cm)	Melting point (°C)
PAN Membrane	328	1.23	280
PP Monolayer	82	0.33	180

thickness on the electrolyte capacity, future experiments will be designed to investigate the effect of Forcespun polymer and nanocomposite membranes on these microstructural properties with the aim to improve the separator performance, mechanical strength, thermal, and shutdown properties.

The absorption and retention of electrolyte although is an important properties of any lithium ion battery separator; however, its ability to withstand the strong oxidation environment in the cell is key. The linear sweep voltammetry results shown in Figure 4 showed that the PAN membrane separator is able to withstand the strong oxidizing positive electrode and the corrosive nature of the electrolyte up to 4.3 V compared to the PP Celgard separator at 3.6 V. The molecular structure as well as the crystallinity of the PAN (Table I) and its favorable interaction with electrolytes species to form various complex compounds[64] is attributed to its chemical stability.

In addition, the increasing vulnerability of the lithium battery to thermal runaway requires a separator with greater mechanical integrity above 130°C[65] to provide a greater margin of safety to the battery. The evaluated thermal properties of both the PAN and PP separators showed that the PAN membrane having a much higher melting temperature of 280°C and crystalline compared to 180°C melting temperature for the PP Celgard separator. These results indicate that the PAN membrane as a separator could maintain its mechanical integrity[36] for high battery operating temperatures and safely shut down its porous structure in the process to prevent cell thermal runaway.

A separator with good electrolyte retention, thermally, and chemically stable will still be required to provide less resistance

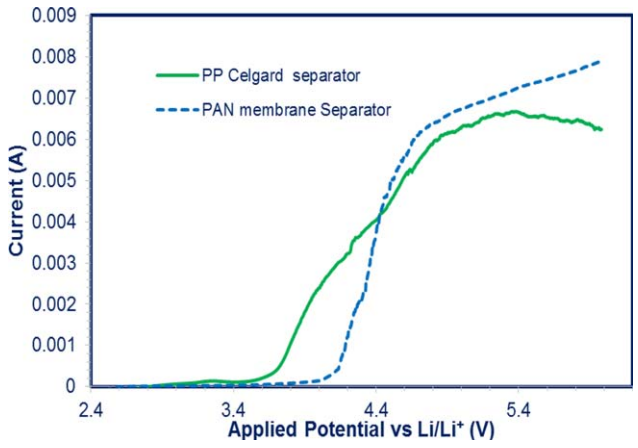

Figure 4. Linear Sweep voltammetry of PAN and PP monolayer separators between the voltage of 2.5 and 6.0 V. [Color figure can be viewed in the online issue, which is available at wileyonlinelibrary.com.]

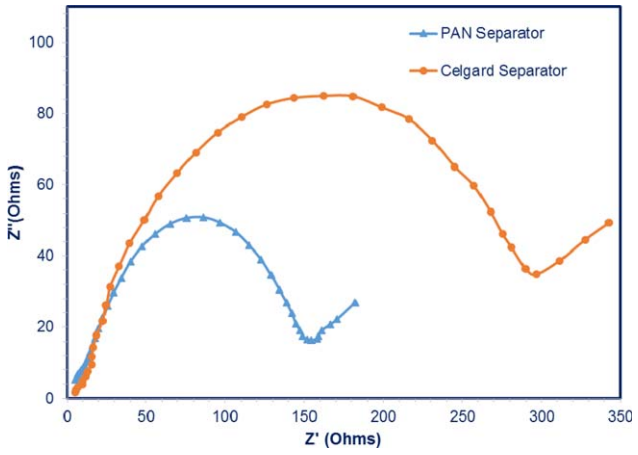

Figure 5. The Nyquist plots for the PAN membrane and PP monolayer separators used in the Li/LiFePO4 cells. [Color figure can be viewed in the online issue, which is available at wileyonlinelibrary.com.]

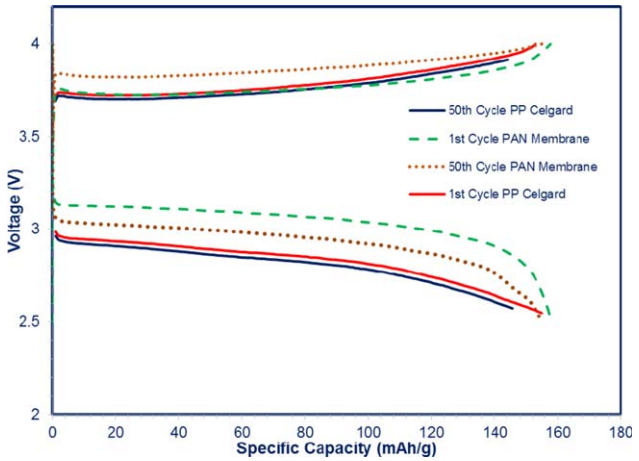

Figure 6. The 1st and 50th cycle charge/discharge capacity of the PAN membrane and PP separator in the Li/LiFePO4 cells. [Color figure can be viewed in the online issue, which is available at wileyonlinelibrary.com.]

at the electrode/separator interface. The electrochemical impedance (EIS) results in Figure 5 show a Nyquist plots for the both the PAN membrane and the PP separators. The radius of the semi-circle indicates the Ohmic resistance in the cell. The PAN membrane, with a smaller semicircle radius, offers less Ohmic resistance in the cell compared with its PP monolayer counterpart. This EIS results translated into better capacity retention and cycling performance for the PAN membrane/$LiFePO_4$ cells relative to the PP microporous membrane separator with a much larger semi-circle radius, meaning a higher Ohmic resistance in the cell.

Cycling Performance

The suitability of the PAN fibrous membrane as a separator for lithium ion batteries was evaluated by assembling a coin cell CR2032 with $LiFePO_4$ as the working electrode and Li metal foil as the counter electrode. Although it is the electrode materials that play a major role in both the energy density and capacity retention of the cell, the separator material directly influences the cell capacity by acting both as the medium of transport of the ions for the electrochemical reaction and a barrier separating the two electrodes.

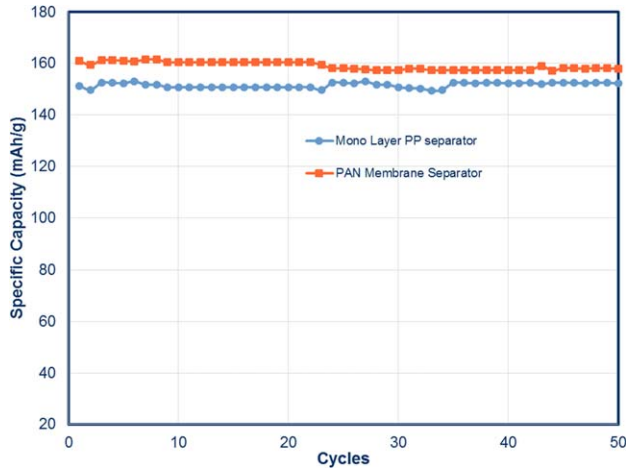

Figure 7. Cycle performance of Li/LiFePO4 cells with PAN membrane compared to those with PP monolayer after 50 cycles. [Color figure can be viewed in the online issue, which is available at wileyonlinelibrary.com.]

As shown in Figures 6 the discharge capacity of the cell using microporous PAN membrane is about 158 mAh g^{-1} for the first discharge cycle compared to 152.mAh g^{-1} for the PP monolayer separator. At the 50th cycle, the PAN membrane had a discharge capacity of about 152 mAh g^{-1} representing capacity retention of about 95% compared 146 mAh g^{-1} capacity for the PP microporous membrane separator. The cycling performance for both the PAN membrane and the PP Celgard separator cells were relatively stable throughout the 50 cycles (Figure 7) with minimal performance degradation. The improved electrochemical performance of the PAN membrane cells is attributed to its higher ionic conductivity, lower interfacial resistance, and higher electrolyte retention that contributed to the enhancement of the electrochemical kinetics at the electrode/separator interface. Thus, allowing easy transport of lithium ions across the interface to enable electrochemical reaction at the electrodes surface. These improved separator indices contributed to making the measured capacity of PAN membrane cells closer to the theoretical value.

CONCLUSIONS

ForceSpinning®, a new cost effective technique for mass producing high quality fibrous mat was employed to produce PAN membrane mats. The method has proven to be a more efficient method that produced a high quality PAN membranes nanofiber that are porous, with high electrolyte retention, ionic conductivity, electrochemical oxidation limit, and interfacial resistance. These properties of the PAN translated into better electrochemical performance of the Li/LiFePO4 cell including better cycling performance and capacity retention compared to the commercially available PP monolayer separator from Celgard Inc. To the best of our knowledge, this is first time a cycling performance for a Forcespun polymer (PAN) nanofibers separator for lithium-ion batteries is being reported. The result from this study is thus the first step to using this technology for the mass production of high quality nanofiber mats made from several polymeric materials as separators for lithium ion batteries. The versatility of the ForceSpining technology makes suitable to extend its application to production nanofiberous mats for electrode material as well as high quality nanofiber for electronics and biosensor applications.

ACKNOWLEDGMENTS

This work was supported by the Startup funding from UT system (STARs Program) to M. Alcoutlabi.

REFERENCES

1. Jiang, H.; Ge, Y. Q.; Fu, K.; Lu, Y.; Chen, C.; Zhu, J. D.; Dirican, M.; Zhang, X. W. *J. Mater. Sci.* **2015**, *50*, 1094.
2. Yanilmaz, M.; Zhang, X. W. *Polymers* **2015**, *7*, 629.
3. Valipouri, A.; Ravandi, S. A. H.; Pishevar, A. R. *Fibers Polym.* **2013**, *14*, 941.
4. Ron, L. Y.; Kotha, S. P. *Mater. Lett.* **2014**, *117*, 153.

5. Arora, P.; Zhang, Z. M. *Chem. Rev.* **2004**, *104*, 4419.
6. Yoshio, M.; Brodd, R. J.; Kozawa, A. Lithium-Ion Batteries: Science and Technologies; Springer: New York, **2009**, *xxvi*, 452 p.
7. Miao, Y. E.; Yan, J. J.; Huang, Y. P.; Fan, W.; Liu, T. X. *Rsc Adv.* **2015**, *5*, 26189.
8. Sethupathy, M.; Sethuraman, V.; Raj, J. A.; Muthuraja, P.; Manisankar, P. *Light Its Interactions Matter* **2014**, *1620*, 253.
9. Zhao, Y. Q.; Wang, H. Y.; Qi, L.; Gao, G. T.; Ma, S. H. *Chinese Chem. Lett.* **2013**, *24*, 975.
10. Tonglairoum, P.; Chaijaroenluk, W.; Rojanarata, T.; Ngawhirunpat, T.; Akkaramongkolporn, P.; Opanasopit, P. *Aaps Pharmscitech.* **2013**, *14*, 838.
11. Kim, Y. J.; Ahn, C. H.; Lee, M. B.; Choi, M. S. *Mater. Chem. Phys.* **2011**, *127*, 137.
12. Gopalan, A. I.; Santhosh, P.; Manesh, K. M.; Nho, J. H.; Kim, S. H.; Hwang, C.-G.; Lee, K.-P. *J. Membr. Sci.* **2008**, *325*, 683.
13. Li, D.; Xia, Y. N. *Adv. Mater* **2004**, *16*, 1151.
14. Yoshikawa, M.; Nakai, K.; Matsumoto, H.; Tanioka, A.; Guiver, M. D.; Robertson, G. P. *Macromol. Rapid Commun.* **2007**, *28*, 2100.
15. Sarkar, K.; Gomez, C.; Zambrano, S.; Ramirez, M.; de Hoyos, E.; Vasquez, H.; Lozano, K. *Mater. Today* **2010**, *13*, 12.
16. Zhang, S. S. *J. Power Sources* **2007**, *164*, 351.
17. Wang, Y.; Travas-Sejdic, J.; Steiner, R. *Solid State Ionics* **2002**, *148*, 3443.
18. Krejci, I.; Vanysek, P.; Trojanek, A. *J. Electrochem. Soc.* **1993**, *140*, 2279.
19. Fang, L. F.; Shi, J. L.; Li, H.; Zhu, B. K.; Zhu, L. P. *J. Appl. Polym. Sci.* **2014**, *131*(21), 41036.
20. Zhang, P.; Chen, L. X.; Shi, C.; Yang, P. T.; Zhao, J. B. *J. Power Sources* **2015**, *284*, 10.
21. Zhang, Z. A.; Zhang, Z. Y.; Li, J.; Lai, Y. Q. *J. Solid State Electrochem.* **2015**, *19*, 1709.
22. Ding, G. L.; Qin, B. S.; Liu, Z. H.; Zhang, J. J.; Zhang, B.; Hu, P.; Zhang, C. J.; Xu, G. J.; Yao, J. H.; Cui, G. L. *J. Electrochem. Soc.* **2015**, *162*, A834.
23. Gao, K.; Hu, X.; Yi, T.; Chen, H. *Acta Polymerica Sinica* **2006**, *9*, 1050.
24. Zhao, Z. Z.; Li, J. Q.; Yuan, X. Y.; Li, X.; Zhang, Y. Y.; Sheng, J. *J. Appl. Poly. Sci.* **2005**, *97*, 466.
25. Huang, X. *J. Solid State Electrochem.* **2011**, *15*, 649.
26. Lee, S. W.; Choi, S. W.; Jo, S. M.; Chin, B. D.; Kim, D. Y.; Lee, K. Y. *J. Power Sources* **2006**, *163*, 41.
27. Lee, S. W.; Choi, S. W.; Jo, S. M.; Chin, B. D.; Kim, D. Y.; Lee, K. Y. *J. Power Sources* **2009**, *189*, 716.
28. Nunes-Pereira, J.; Costa, C. M.; Lanceros-Mendez, S. *J. Power Sources* **2015**, *281*, 378.
29. Yanilmaz, M.; Chen, C.; Zhang, X. W. *J. Polym. Sci. Part B-Polym. Phy.* **2013**, *51*, 1719.
30. Cho, T. H.; Tanaka, M.; Ohnishi, H.; Kondo, Y.; Yoshikazu, M.; Nakamura, T.; Sakai, T. *J. Power Sources* **2010**, *195*, 4272.
31. Lee, Y. M.; Kim, J. W.; Choi, N. S.; Lee, J. A.; Seol, W. H.; Park, J. K. *J. Power Sources* **2005**, *139*, 235.
32. Li, S. L.; Ai, X. P.; Yang, H. X.; Cao, Y. L. *J. Power Sources* **2009**, *189*, 771.
33. Lee, Y. S.; Jeong, Y. B.; Kim, D. W. *J. Power Sources* **2010**, *195*, 6197.
34. Alcoutlabi, M.; Banda, L.; McKenna, G. B. *Polymer* **2004**, *45*, 5629.
35. Alcoutlabi, M.; Banda, L.; Kollengodu-Subramanian, S.; Zhao, J.; McKenna, G. B. *Macromolecules* **2011**, *44*, 3828.
36. Alcoutlabi, M.; Lee, H.; Watson, J. V.; Zhang, X. W. *J. Mater. Sci.* **2013**, *48*, 2690.
37. Lee, H.; Alcoutlabi, M.; Toprakci, O.; Xu, G. J.; Watson, J. V.; Zhang, X. W. *J. Solid State Electrochem.* **2014**, *18*, 2451.
38. Lee, H.; Alcoutlabi, M.; Watson, J. V.; Zhang, X. W. *J. Appl. Polym. Sci.* **2013**, *129*, 1939.
39. Lee, H.; Alcoutlabi, M.; Watson, J. V.; Zhang, X. W. *J. Polym. Sci. Part B-Polym. Phys.* **2013**, *51*, 349.
40. Liang, Y. Z.; Ji, L. W.; Guo, B. K.; Lin, Z.; Yao, Y. F.; Li, Y.; Alcoutlabi, M.; Qiu, Y. P.; Zhang, X. W. *J. Power Sources* **2011**, *196*, 436.
41. Weng, B. C.; Xu, F. H.; Alcoutlabi, M.; Mao, Y. B.; Lozano, K. *Cellulose* **2015**, *22*, 1311.
42. Weng, B. C.; Xu, F. H.; Garza, G.; Alcoutlabi, M.; Salinas, A.; Lozano, K. *Polym. Eng. Sci.* **2015**, *55*, 81.
43. Juang, R.-S.; Hsieh, C.-T.; Chen, P.-A.; Chen, Y.-F. *J. Power Sources* **2015**, *286*, 526.
44. Choi, J. A.; Kim, S. H.; Kim, D. W. *J. Power Sources* **2010**, *195*, 6192.
45. Jeong, H. S.; Lee, S. Y. *J. Power Sources* **2011**, *196*, 6716.
46. Yanilmaz, M.; Lu, Y.; Li, Y.; Zhang, X. W. *J. Power Sources* **2015**, *273*, 1114.
47. Kim, Y. J.; Kim, H. S.; Doh, C. H.; Kim, S. H.; Lee, S. M. *J. Power Sources* **2013**, *244*, 196.
48. Khan, W. S.; Asmatulu, R.; Rodriguez, V.; Ceylan, M. *Int. J. Energy Res.* **2014**, *38*, 2044.
49. Lee, H.; Yun, J.; Choi, H.; Kim, D.; Byun, H. *Appl. Energy Technol.* **2013**, *724725*, 1079.
50. Dabirian, F.; Ravandi, S. A. H.; Pishevar, A. R. *Current Nanosci.* **2010**, *6*, 545.
51. Yao, Y. F.; Lin, Z.; Li, Y.; Alcoutlabi, M. *Adv. Energy Mater.* **2011**, *1*, 1133.
52. Zhou, X. H.; Yue, L. P.; Zhang, J. J.; Kong, Q. S.; Liu, Z. H.; Yao, J. H.; Cui, G. L. *J. Electrochem. Soc.* **2013**, *160*, A1341.
53. Sohn, J. Y.; Im, J. S.; Gwon, S. J.; Choi, J. H.; Shin, J.; Nho, Y. C. *Radiat. Phys. Chem.* **2009**, *78*, 505.
54. Sohn, J. Y.; Im, J. S.; Shin, J.; Nho, Y. C. *J. Solid State Electrochem.* **2012**, *16*, 551.
55. Aravindan, V.; Sundaramurthy, J.; Kumar, P. S.; Shubha, N.; Ling, W. C.; Ramakrishna, S.; Madhavi, S. *Nanoscale* **2013**, *5*, 10636.
56. Cao, C. Y.; Tan, L.; Liu, W. W.; Ma, J. Q.; Li, L. *J. Power Sources* **2014**, *248*, 224.
57. Khamforoush, M.; Asgari, T. *Nano* **2015**, *10*, 2.

58. Dabirian, F.; Ravandi, S. A. H.; Pishevar, A. R.; Abuzade, R. A. *J. Electrostat.* **2011**, *69*, 540.

59. Dabirian, F.; Ravandi, S. A. H.; Pishevar, A. R. *Fibers Polym.* **2013**, *14*, 1497.

60. FibeRiO. Information on L1000 Forcespinning, at: http://fiberiotech.com/ (accessed June 28, 2015).

61. Hong, C. K.; Yang, K. S.; Oh, S. H.; Ahn, J. H.; Cho, B. H.; Nah, C. *Polym. Int.* **2008**, *57*, 1357.

62. Wang, S. H.; Hou, S. S.; Kuo, P. L.; Teng, H. *ACS Appl. Mater. Interfaces* **2013**, *5*, 8477.

63. Jiang, W.; Liu, Z. H.; Kong, Q. S.; Yao, J. H.; Zhang, C. J.; Han, P. X.; Cui, G. L. *Solid State Ionics* **2013**, *232*, 44.

64. Mihut, D. M.; Lozano, K.; Foltz, H. *J. Vacuum Sci. Technol. A* **2014**, *32*,

65. Weng, B. C.; Xu, F. H.; Lozano, K. *J. Appl. Polym. Sci.* **2014**, 1311.